JBIC (1997) 2:492–506

ORIGINAL ARTICLE

Zeev Gross · Shay Nimri · Claudia M. Barzilay
Liliya Simkhovich

Reaction profile of the last step in cytochrome P-450 catalysis revealed by studies of model complexes

Received: 16 January 1997 / Accepted: 24 May 1997

Abstract A series of oxoiron(IV) porphyrin cation radical complexes was investigated as compound I analogs of cytochrome P-450. Both the spectroscopic features and the reactivities of the complexes in oxygen atom transfer to olefins were examined as a function of only one variable, the axial ligand *trans* to the oxoiron(IV) bond. The results disclosed two important kinetic steps – electron transfer from olefin to oxoiron(IV) and intramolecular electron transfer from metal to porphyrin radical – which are affected differently by the axial ligands. The large kinetic barrier of the latter step in the reaction of olefins with the perchlorato-bound oxoiron(IV) porphyrin cation radical complex enabled the trapping of a reaction intermediate in which the metal, but not the porphyrin radical, is reduced. The first electron transfer step is probably followed by σ-bond formation, which readily accounts for formation of isomerized organic products at low temperatures. It is finally postulated that part of the enhanced oxygenation activities of cytochrome P-450 monooxygenases and chloroperoxidases is due to a lowering of the energy barrier for the second electron transfer step via participation of their redox-active cysteinate ligand.

Key words Cytochrome P-450 · Compound I · Heme enzymes · Oxoiron · Porphyrin cation radicals

Abbreviations *HRP* horseradish peroxidase · *CCP* cytochrome *c* peroxidase · *CAT* catalases · *CPO* chloroperoxidases · *TMP* tetramesitylporphyrin dianion · TMP^+ · one-electron-oxidized TMP (tetramesitylporphyrin cation radical)

Z. Gross (✉) · S. Nimri · C. M. Barzilay · L. Simkhovich
Department of Chemistry,
Technion – Israel Institute of Technology,
Haifa 32000, Israel
Tel.: +972-4-8293954; Fax: +972-4-8233735;
e-mail: chr10zg@tx.technion.ac.il

Introduction

The ubiquitousness and the variety of the natural functions of hemoproteins has led to intensive investigation of their structural and mechanistic aspects on multi- and interdisciplinary levels. An integral part of research in this field is the investigation of relatively simple synthetic metalloporphyrins, which have a serious impact on our current understanding of the intriguing phenomena involved in the biological systems. The best known examples are Collman's picket-fence porphyrins [1], whose contribution to the subject of reversible binding of molecular oxygen by myo- and hemoglobin is nowadays mentioned in all modern textbooks of Chemistry and Biology. A major advantage of model compounds is the fact that the modification required to achieve control of the identity of the metal, its spin, oxidation, and coordination states, and other variables is relatively easy [2]. In addition, the high symmetry of the complexes significantly assists in spectroscopic analysis.

One outstanding class within the large family of hemoproteins includes cytochrome P-450 enzymes [3], which have several unique properties. These are the only hemoproteins to utilize molecular oxygen as the oxygen atom source for oxygenation; the heme of their active site is coordinated to a cysteinate side chain – a property shared only with chloroperoxidases (CPO) [4]; their catalytic cycle contains a reductive part; and they catalyze an exceptionally large number of chemically distinctively different reactions [5]. The dual role of P-450 in biodegradation and biosynthesis, as well as the very efficient synthetic oxidation catalysts which were developed based on the principles behind these reactions [6, 7], puts the research of model compounds of P-450 at the forefront of scientific interest [8].

The elementary steps of the catalytic cycle of P-450 are well known (Scheme 1), although none of the proposed high-valency intermediates was ever isolated to enable thorough spectroscopic characterization [9].

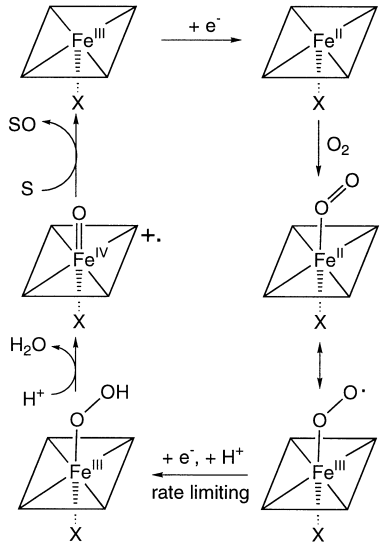

Scheme 1 The catalytic cycle of cytochrome P-450

Since the rate-limiting step in P-450 catalysis is the decomposition of the oxy-complex, most of the information was not derived from direct studies on cytochrome P-450, but rather from either related enzymes or synthetic model complexes. The oxygen atom transfer intermediate is generally considered to have a compound I structure similar to that of peroxidases [horseradish peroxidase (HRP) and cytochrome *c* peroxidase (CCP)], catalases (CAT), and CPO. The definition of compound I is "two oxidation states higher than the iron(III) porphyrin resting state", but distinct differences between the various compounds I are well documented. They all have in common an oxoiron(IV) moiety, while the additional oxidation equivalent is located either on the protein (CCP) [10] or on the porphyrin (HRP [11], CAT, CPO [12], model complexes [13]). Ongoing research is focussed on elucidation of the variables which determine the mode and strength of the intramolecular spin-spin interactions between the unpaired electrons on the metal and the porphyrin radical [14]. Related open questions are concerned with the effect of the cysteinate ligand in P-450 on the electronic structure of its compound I and on the oxoiron(IV) bond strength, and the reaction mechanism of compound I with olefins, which is the last step in the catalytic conversion of olefins to epoxides. Direct answers to these questions may well remain elusive forever, because of the impossibility of characterizing the compound I of P-450 enzymes. Because of this, resolution of these aspects via utilization of synthetic model complexes of P-450 has been the subject of many studies during the last two decades [15].

A major breakthrough in this regard was the isolation and characterization of the first synthetic compound I analog, achieved by Groves et al. via the *m*-CPBA (3-chloroperoxybenzoic acid) oxidation of (TMP)FeCl [16]. This intermediate was identified as an oxoiron(IV) porphyrin cation radical complex, $[(TMP^{+}\cdot)Fe^{IV}(O)]^{+}$ (**1**), based on UV-vis [16], NMR [16], Mössbauer [16], EPR [17], resonance Raman (RR) [18, 19], and EXAFS [20] spectroscopies. Similar to compounds I of the various enzymes, complex **1** is a cationic complex with an additional axial ligand *trans* to the oxo ligand. That this distinction is real and not semantic was shown for the synthetic complexes via NMR investigations by the groups of Groves [21], Balch [22], and Gross [23]. In heme-dependent enzymes, the apoprotein provides the axial ligand, which is histidine for peroxidases, tyrosinate for catalases, and cysteinate for CPO and P-450 (see [24] and references therein). As this is the only difference between the prosthetic groups in these enzymes, many research groups have searched for an effect of the axial ligands on the oxo-iron(IV) bond strength and length. In the absence of a crystal structure for any porphyrin-oxidized compound I [25], emphasis was given to EXAFS and vibronic spectroscopies. The existing EXAFS data is quite surprising, as a bond length of 1.65 ± 0.05 Å was obtained not only for various compounds I, but also for compound II and its synthetic model complexes, in which the porphyrin is not oxidized[1] [4, 26]. It thus appears that the Fe=O bond length is not sensitive to (a) the identity of the *trans*-axial ligand, (b) the identity of its porphyrin ligand, protoporphyrin IX (HRP, CAT, CPO, and CCP), heme *a* (beef heart cytochrome *c* oxidase) or synthetic porphyrin, or (c) the oxidation state of its porphyrin ligand. A more sensitive method for monitoring the Fe=O bond strength in the enzymes would be the determination of its stretching frequency by RR spectroscopy. However, quite different values of ν(Fe=O) were obtained in the various reports. Thus, 737 and 791 cm^{-1} were reported for compound I of HRP [27, 28], 767 and 753 cm^{-1} for compound I of CCP [29, 30], and 788–775 cm^{-1} for ν(Fe=O) of compound II of HRP (depending on the pH) [31]. The major problems in these examinations were the photosensitivity of the complexes [19], the identity of the axial ligand *trans* to the oxoiron(IV) bond under different conditions such as pH, and the presence or absence of alcoholic co-solvents [32].

To elucidate the functional modelling of P-450 enzymes (catalytic oxygenation of hydrocarbons), the mechanism of hydroxylation of alkanes and epoxidation of olefins under metalloporphyrin catalysis was extensively investigated by indirect methods (kinetics, product distribution, radical clocks, etc.) by many research groups [8]. Most observations in hydroxylation reactions are well accommodated by the rebound mechanism shown in Scheme 2 [33]. However, epoxidation of olefins by these systems proceeds by a completely different mechanism. This includes also substrates such as cyclohexene, for which epoxidation and

[1] A few exceptional cases with much longer bond lengths were also reported, but are attributed to either experimental pitfalls or unconventional data analysis

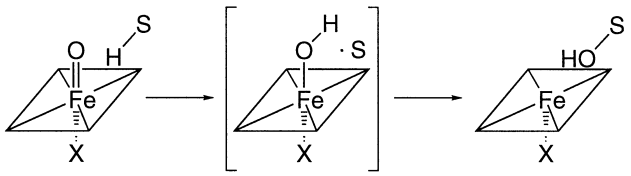

Scheme 2 The rebound mechanism for hydroxylation of alkanes by oxoiron(IV) porphyrin cation radical complexes

hydroxylation could in principle proceed through one common intermediate [34]. Although it is generally accepted that intermediates which contain both the high-valency metalloporphyrin and the olefin must exist on the pathway to the final products (iron(III) porphyrin and the oxygenated substrate), there is no consensus about the structure of these intermediates. The most common proposals are metallacycle [35, 36], charge transfer [37], electron transfer [38], or radical complexes [39] (Scheme 3). Interestingly, similar intermediates are frequently suggested to accommodate results of transition-metal-catalyzed epoxidation reactions in completely inorganic systems [40]. In only one case was the *direct* observation of an intermediate achieved, but, because the spectroscopic characterization was limited to UV-vis, no clear-cut structural elucidation was possible [41].

In a series of three short publications we have attacked the above-mentioned open questions in a systematic way. First, by monitoring the rate of epoxidation of styrene by complexes of **1** with various axial ligands [23] we have shown that the reactivity of synthetic analogs of compound I can be modulated by the ligands *trans* to the Fe=O bond. Consequently, we have succeeded in the trapping and spectroscopic characterization of a reaction intermediate [42]. Finally, we were able to demonstrate an intriguing effect of axial ligands on the Fe=O bond strength in oxoiron(IV) porphyrin cation radicals by RR spectroscopy [43]. We are now presenting a full report of these and new observations which lead to elucidation of a detailed reaction profile for the reaction of synthetic analogs of compound I with olefins. All evidence is fully consistent with a multi-step mechanism, in which electron transfer from olefin to the Fe=O moiety is followed by σ-bond formation between oxygen and olefin radical, intramolecular rearrangement of the electronic structure, and release

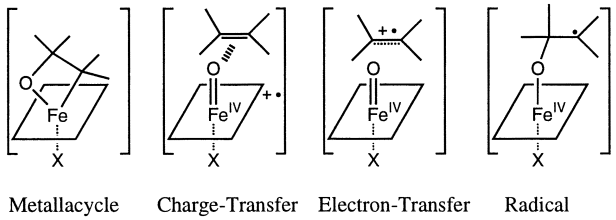

Scheme 3 The proposed intermediates in epoxidation of alkenes by oxoiron(IV) porphyrin cation radical complexes

of the products. It is shown that the major kinetic effect of the axial ligands is on the intramolecular electron transfer from iron(III) to porphyrin radical.

Materials and methods

The instrumental details and other routine methods are identical to those outlined in a recent publication [44]. Purification of solvents and preparation of the iron(III) tetramesitylporphyrins with different axial ligands [(TMP)Fe^{III}-X, **2**-X] are also described therein.

Preparation of iron(III) porphyrin cation radical and manganese(IV) porphyrin complexes

$(TMP^{+}\cdot)Fe^{III}(ClO_4)_2$

This known complex was prepared by the procedure of Groves et al. [45]. UV-vis (CH_2Cl_2, RT) λ_{max} (nm) 394 (Soret), 616, 656 (Q bands); ^{1}H NMR (200 MHz, $CDCl_3$, RT) δ (ppm) 13.2 (12 H, *para*-CH_3), 21.0 (24 H, *ortho*-CH_3), 26.6 (8 H, *pyrrole*-H), 57.6 (8 H, *meta*-H).

$(TMP^{+}\cdot)Fe^{III}(Cl)(SbCl_6)$

This complex was obtained by oxidation of (TMP)Fe(Cl) with the hexachloroantimonate salt of phenoxathiine cation radical following the established procedure for preparation of $(TTP^{+}\cdot)Fe(Cl)(SbCl_6)$ and $(TTP^{+}\cdot)Fe(Cl)(SbCl_6)$ [46]. UV-vis (CH_2Cl_2, RT) λ_{max} (nm) 374 (Soret), 548 (Q bands); ^{1}H NMR (200 MHz, $CDCl_3$, RT) δ (ppm) −27.7 (8 H, *meta*-H), −9.8 (12 H, *ortho*-CH_3), −6.9 (12 H, *ortho*-CH_3), −5.0 (12 H, *para*-CH_3), 68.8 (8 H, *pyrrole*-H).

$(TMP^{+}\cdot)Fe^{III}(OAc)_2$

First, the acetate salt of dibenzo-*p*-dioxin cation radical was prepared by the following procedure. Dibenzo-*p*-dioxin (40 mg) was dissolved in an ice-cooled acetic anhydride solution containing tetrabutyl ammonium acetate (0.05 M). Solid CrO_3 (5 mg) was added and, after vigorously stirring for a few minutes, the solution was filtered in order to remove any undissolved CrO_3. One to two drops of conc. $HClO_4$ were added, which caused an immediate appearance of a deep blue color and precipitation of the salt. The product was isolated by filtration and washed three times with acetic anhydride and twice with CH_2Cl_2. The oxidant was finally dried under high vacuum for 1 h and, because of its instability, was used within 5 h of its preparation.

The $(TMP^{+}\cdot)Fe^{III}(OAc)_2$ complex was prepared by adding 1.2 equivalents of the acetate salt of dibenzo-*p*-dioxin cation radical in one portion to a well-stirred solution of (TMP)Fe(OAc) in CH_2Cl_2. After the color change to brilliant green was complete (minutes), the solution was filtered and the product was precipitated by the addition of cold heptane. The product $(TMP^{+}\cdot)Fe^{III}(OAc)_2$ was isolated and dried under high vacuum. UV-vis (CH_2Cl_2, RT) λ_{max} (nm) 394 (Soret), 628, 680 (Q bands); ^{1}H NMR (200 MHz, $CDCl_3$, RT) δ (ppm) 13.1 (12 H, *para*-CH_3), 20.9 (24 H, *ortho*-CH_3), 26.0 (8 H, *pyrrole*-H), 57.1 (8 H, *meta*-H).

$(TMP)Mn^{IV}(Cl)_2$

This complex was prepared via ligand exchange (which also caused change in the oxidation site from porphyrin to manganese) of the perchlorato ligands in $(TMP^{+}\cdot)Mn^{III}(ClO_4)_2$ by chloride anions. The preparation and full characterization of both

$(TMP^{+}\cdot)Mn^{III}(ClO_4)_2$ and $(TMP)Mn^{IV}(Cl)_2$ are reported in a separate recent publication [47].

Preparation and characterization of oxoiron(IV) tetramesitylporphyrin cation radical complexes with different axial ligands (**1**-X; X = F^-, Cl^-, AcO^-, CH_3OH, $CF_3SO_3^-$, ClO_4^-)

Solutions of **1**-X were obtained by bubbling ozone at −78 °C for 30 s (6 μmol O_3/min, 1.1 equiv.) into 2.6 μmol of the dissolved **2**-X (0.6 mL CD_2Cl_2 for NMR and EPR measurements, 1.5 mL CH_2Cl_2 for the kinetic experiments), followed by purging with N_2 (70 mL/min) for 1 min. The complex **1**-$HOCH_3$ was obtained by oxidation of **2**-Cl in CH_2Cl_2 (CD_2Cl_2) which contained 5% MeOH (MeOH-d_4). The spectroscopic data of the complexes are summarized in Tables 1 and 2.

Kinetic investigation of the stoichiometric oxidation of styrene by **1**-X

Solutions of **1**-X at −78 °C were prepared as described in the previous paragraph. After the oxidation was complete, excess ozone and oxygen were removed by nitrogen purging and 1 equiv. nitrobenzene was added as internal standard. Next, 30–400 equiv. styrene were added at once under a constant stream of N_2, which was kept on during the reactions. Small aliquots were removed from the reaction vessel and quenched by an excess of *n*-Bu_4NI, still at −78 °C. These aliquots were examined by GC analysis relative to the internal standard. For each of the various **1**-X compounds, 6–8 aliquots were examined at different time intervals, covering about $2t_{1/2}$. An additional aliquot was examined much later to obtain a reliable infinity point. Only styrene oxide was detected, and its formation followed excellent pseudo-first-order kinetics. The second-order rate constants for these reactions were elucidated from the linear dependence of the pseudo-first-order rate constants on the concentrations of styrene (five different concentrations were used for each **1**-X). The yields of styrene oxide relative to **1**-X were calculated from the equation: Yield $= 100 \times k[\text{styrene}]/k_{obs}$, where k is the second order rate constant (Table 3) and k_{obs} are the pseudo-first-order constants for particular concentrations of styrene.

Product ratio for epoxidation of cis-β-methylstyrene

Epoxidation of *cis*-β-methylstyrene was carried out at various reaction conditions with special emphasis on the product ratio of the *cis*- to the *trans*-β-methylstyrene oxides. Special attention was given to the possibility of product isomerization during gas chromatographic analysis by checking reference solutions of *cis*-β-methylstyrene oxide at the beginning and the end of the examinations. The following reaction conditions were employed: stirring a solution of 0.1–0.13 mL *cis*-β-methylstyrene (0.8–1.0 mmol), 80–120 mg iodosylbenzene (0.36–0.56 mmol), and 0.6–1.0 mg (TMP)Fe-X (0.7–1.1 μmol) in 8 mL solvent for 1 h followed by bulb-to-bulb distillation and GC analysis. The product ratio was in the range of 96–98.5% *cis*-oxide for catalysis by (TMP)Fe-Cl, (TMP)Fe-F, and (TMP)Fe-CO_4 at 25 °C (both in CH_2Cl_2 and benzene) and 0 °C (CH_2Cl_2). The same reaction conditions were also applied at −78 °C in CH_2Cl_2 with (TMP)Fe-Cl as catalyst. Because of the low temperature, the reaction proceeded to only a small extent. In order to avoid continuation of the reaction at higher temperature during the workup procedure, the bulb-to-bulb distillation was carried out at −78 °C. The product ratio was very different, in favor of the *trans* isomer, with *cis/trans* ratios in the range 0.19–0.23 for three different runs. Stoichiometric reactions were performed by dissolving 1.0–1.2 mg (1.1–1.37 μmol) of (TMP)Fe-X, X = Cl, F, ClO_4, in 1 mL of CH_2Cl_2. First the **2**-X complexes were oxidized by ozone to **1**-X, and this was followed by an N_2 purge and addition of the olefin. The *cis/trans* epoxide ratios were 0.88, 0.50, and 0.63 for X = Cl, F, and ClO_4, respectively. The same reaction conditions were also applied with 1.2 equiv of *m*-CPBA as oxidant for the transformation of **2**-X to **1**-X. In CH_2Cl_2 solution the *cis/trans* epoxide ratio was 0.42–0.50, while a ratio of 2.6 was obtained under identical reaction conditions in a solution of 7% MeOH in CH_2Cl_2.

Results

Preparation of oxoiron(IV)tetramesitylporphyrin cation radical complexes with different axial ligands (**1**-X)

The series of iron(III) tetramesitylporphyrins with different axial ligands [(TMP)Fe-X, **2**-X; X = F^-, Cl^-, AcO^-, $CF_3SO_3^-$ (trif$^-$), ClO_4^-] were oxidized by ozone at −78 °C to the corresponding oxoiron(IV) tetramesitylporphyrin cation radical complexes (**1**-X, Scheme 4). The complex **1**-MeOH was obtained by oxidation of **2**-Cl in CD_2Cl_2 which contained 5% MeOH-d_4. The EPR spectra of all complexes as frozen solutions were obtained at 15 K in order to verify that oxoiron(IV) porphyrin cation radicals were indeed formed by this procedure. The characteristic $S = 3/2$ EPR spectrum of **1**-$OClO_3$, which is representative of the spectra of all other complexes, is presented in Fig. 1 of our previous publication [23]. As can be seen from the data summarized in Table 1, the effect of the axial ligands on the g values was only minor. The ^{1}H NMR spectra of all complexes were obtained also, in CD_2Cl_2 solutions at −80 °C. The chemical shifts are presented in Table 2, and three examples were have been given previously [23]. It is clear that the axial ligands had a significant effect on the chemical shifts, although the general pattern (*pyrrole*-H upfield, all others downfield), characteristic for this type of compounds, was preserved. The

Table 1 EPR data ($g_z = 2$ for all complexes) for the various oxoiron(IV) tetramesitylporphyrin cation radical complexes **1**-X at 15 K in frozen CD_2Cl_2

	1-F	**1**-MeOH	**1**-Cl	**1**-OAc	**1**-Trif	**1**-ClO_4
g_x	4.34	4.29	4.23	4.32	4.31	4.33
g_y	3.56	3.56	3.72	3.70	3.54	3.56

Table 2 ^{1}H NMR data (δ, ppm) for the various oxoiron(IV) tetramesitylporphyrin cation radical complexes **1**-X in CD_2Cl_2 at −80 °C

X in **1**-X	*meta*-H	*ortho*-CH_3	*para*-CH_3	*pyr*-H
F^-	71.4	26.9, 42.1	10.7	−13.0
MeOH	69.4	26.7, 24.1	11.2	−26.7
Cl^-	60.6	23.3, 20.2	10.7	− 6.7
AcO^-	76.2	25.7, 28.5	11.3	− 8.3
trif$^-$	68.6	26.8, 24.3	11.3	−26.2
ClO_4^-	65.3	26.0, 23.5	11.1	−26.9

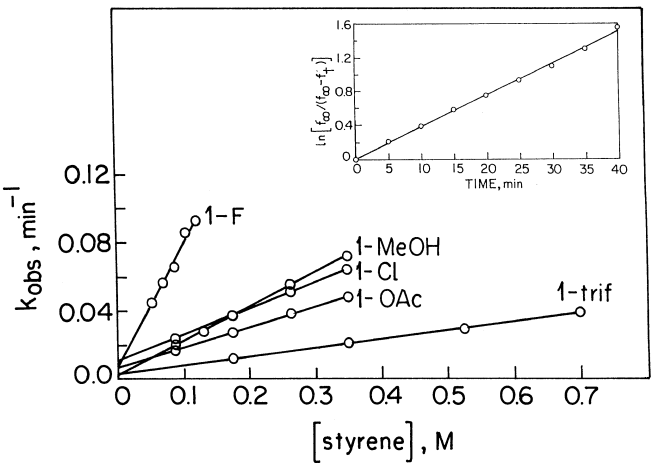

Fig. 1 Plot of the pseudo-first-order reaction constants (k_{obs}) for the reactions of styrene with the various oxoiron(IV) tetramesitylporphyrin cation radical complexes (**1**-X, Scheme 5) as a function of the concentration of styrene at −78 °C in CH_2Cl_2. *Inset:* Time-dependent formation of styrene oxide in the reaction of **1**-Cl with 0.175 M styrene as a representative example of the reaction kinetics utilized to obtain one particular pseudo-first-order reaction constant (k_{obs})

spectroscopic characterization not only served to confirm the formation of oxoiron(IV) porphyrin cation radicals by this procedure, but also to eliminate the possibility of other reactive species [48, 49].

Kinetic investigation of the stoichiometric oxidation of styrene by **1**-X

The high yield of styrene oxide obtained by addition of excess styrene to preformed solutions of **1**-X at −78 °C followed excellent pseudo-first-order kinetics, as shown for one example in the inset of Fig. 1. The second-order rate constants for these reactions were elucidated from the linear dependence of the pseudo-first-order rate constants on the concentrations of styrene, as shown in Fig. 1. The results, which are collected in Table 3, revealed a pronounced ligand effect on the reactivity of **1**-X toward styrene; the reaction of **1**-F was 15 times faster than that of **1**-trif, and no organic products were obtained in the reaction of **1**-$OClO_3$.

Table 3 The second-order rate constants for reaction of the various oxoiron(IV) tetramesitylporphyrin cation radical complexes **1**-X with styrene at −78 °C in CH_2Cl_2

X in **1**-X	F^-	MeOH	Cl^-	AcO^-	$trif^-$	ClO_4^-
k ($M^{-1}\,h^{-1}$)[a]	42.4	11.8	8.9	6.8	2.8	0[b]

[a] ±5%
[b] No organic products were formed

^{1}H NMR investigation of the reactions of styrene with **1**-X

*With **1**-$OClO_3$*

The addition of 100 equivalents of styrene-d_8 to an N_2-purged solution of **1**-$OClO_3$ in CD_2Cl_2 at −80 °C resulted in the spectral change shown in Fig. 3 (the spectrum of **1**-$OClO_3$ changed to that of **3**-$OClO_3$, see discussion) at a rate which was dependent on the amount of styrene added. Identical results were obtained with regular styrene and saturation of its signals. The assignment of resonances to particular protons in **3**-$OClO_3$ was achieved by utilizing deuterated porphyrins, as outlined in the discussion. No further reaction occurred for many hours, and no organic products were detected by GC if such solutions were quenched by n-Bu_4NI at −78 °C. A solution of complex **3**-$OClO_3$, prepared by addition of 100 equivalents of styrene to **1**-$OClO_3$, was left at −78 °C for 13 h. Subsequently, it was warmed up in the NMR probe in 10 °C intervals. The **3**-$OClO_3$ complex was stable up to −30 °C, where it slowly converted to the original **2**-$OClO_3$. GC analysis of that solution showed that styrene oxide (17%) and phenylacetaldehyde (5%) were formed. In a similar experiment, 100 equivalents of styrene and 0.1 equivalents of nitrobenzene were added to a solution of **1**-$OClO_3$ in CH_2Cl_2 at −78 °C under N_2. Small aliquots were removed from the solution by a gas-tight syringe 15, 25, and 35 min after the addition of styrene. GC examinations were performed after the samples were left at room temperature for 4 min (the color changed from green to violet) in the syringe. The yields of organic products were 65, 65, and 58% with a ratio of styrene oxide/phenylacetaldehyde of 1.3, 1.6, and 0.9, respectively.

*With **1**-$OClO_3$ followed by addition of CD_3OD*

Addition of 20 μL CD_3OD (5% v/v) to a solution of **3**-$OClO_3$, preformed by adding 60 equivalents of styrene to an N_2-purged **1**-$OClO_3$ solution at −78 °C (Fig. 4a), resulted in the spectrum shown in Fig. 4b. The NMR spectrum of this solution changed gradually at −80 °C. After 1 h, the spectrum shown in Fig. 4c was obtained. GC examination of this solution revealed the production of 24% styrene oxide and 20% phenylacetaldehyde (based on the amount relative to nitrobenzene added after the end of the reaction).

*With **1**-trif*

In a similar NMR experiment, 100 equivalents of styrene-d_8 were added to a solution of **1**-trif. A complex (**3**-trif) with spectrum similar to that of **3**-$OClO_3$ was formed, and both **1**-trif and **3**-trif decayed slowly to **2**-trif at −80 °C.

*With **1**-Cl*

With **1**-Cl as starting material and 30 equivalents of styrene-d_8, the transformation to **2**-Cl proceeded at −80 °C, no other complex being observed.

Preparation and characterization of one-electron-oxidized iron(III) and manganese(III) tetramesitylporphyrin complexes

The site of oxidation (porphyrin or metal) in the one-electron oxidation products was identified by the well-established distinctly different spectroscopic features of metal(III) porphyrin cation radicals and metal(IV) porphyrins [50]. The known complex $(TMP^{+}\cdot)Fe^{III}(ClO_4)_2$ was prepared by oxidation of $(TMP)Fe^{III}(ClO_4)$ with $Fe(ClO_4)_3$ as previously described [44], while $(TMP^{+}\cdot)Fe^{III}(Cl)(SbCl_6)$ was obtained by oxidation of $(TMP)Fe^{III}(Cl)$ with the hexachloroantimonate salt of phenoxathiine cation radical via an established procedure and identified by comparison of its UV-vis and NMR spectra with those of similar complexes such as $(TPP^{+}\cdot)Fe^{III}(Cl)(SbCl_6)$ and $(TTP^{+}\cdot)Fe^{III}(Cl)(SbCl_6)$ [46]. Similarly, $(TMP^{+}\cdot)Fe^{III}(OAc)_2$ was prepared from $(TMP)Fe^{III}(OAc)$ via its oxidation by the acetate salt of phenoxathiine cation radical. Its identification as a porphyrin cation radical was based on its green color, blue-shifted and reduced-intensity Soret band, new red-shifted visible bands, and ^1H NMR spectrum, which is similar to that of $(TMP^{+}\cdot)Fe^{III}(ClO_4)_2$ and very different from that of $(TMP)Fe^{IV}(OCH_3)_2$ [50]. The $(TMP^{+}\cdot)Mn^{III}(ClO_4)_2$ complex was prepared by oxidation of $(TMP)Mn^{III}(ClO_4)$ with $Fe(ClO_4)_3$ and identified by comparison of its spectroscopic characteristics to those previously reported. Treatment of $(TMP^{+}\cdot)Mn^{III}(ClO_4)2$ with tetraethylammonium chloride resulted in a color change from green to red, and the isolated product was characterized as $(TMP)Mn^{IV}(Cl)_2$ by various spectroscopic methods [47].

Discussion

The research goals of these studies were: (a) to study the effect of different axial ligands on the spectroscopic features of synthetic analogs of P-450's compound I, with particular emphasis on the oxo-iron(IV) bond strength, (b) to examine the effect of the same axial ligands on the rate of epoxidation of olefins by the complexes, and (c) to search for a structure-reactivity relationship in order to throw some light on the mechanism of these reactions. We decided to concentrate on oxo-iron(IV) tetramesitylporphyrin cation radical complexes, **1**-X, where **1** stands for the cationic complex and X for the axial ligand *trans* to the oxo-iron bond. The tetramesitylporphyrin ligand was preferred over the more robust phenyl- and/or pyrrole-halogenated derivatives because of the high solubility of its metal complexes, its rich ^1H NMR features, and the relatively high stability of its complexes with high-valency iron.

Preparation of the **1**-X complexes and structural proofs

A priori, the **1**-X complexes should be accessible via the standard *m*-CPBA oxidation of the corresponding iron(III) complexes (**2**-X) [16]. In our hands, however, a mixture of **1** with various axial ligands was formed by this procedure, as confirmed by NMR. Repeating the same procedure in CD_2Cl_2/5% CD_3OD resulted in very pure solutions of **1** but with CD_3OD as the axial ligand (see also the reports of Groves [21] and Balch [22]). Accordingly, we searched for an oxidant which, unlike *m*-CPBA, amine-*N*-oxides, and iodosylbenzene, will not replace the original axial ligand either itself or as its reduced product (*m*-CBA or amines). Ozone, whose utilization as oxidant for iron(III) porphyrins was previously demonstrated by Sawyer [51], appeared to be ideal for this purpose, since neither ozone nor molecular oxygen – the precursor and the byproduct of ozone – are potential ligands of the high-valency metal complex. In accord with these expectations, pure solutions of **1**-X were indeed obtained by this procedure (Scheme 4).

The formation of oxoiron(IV) porphyrin cation radical complexes with different axial ligands was assured by a combination of several spectroscopic methods. The color change to brilliant green upon oxidation of the iron(III) porphyrins and the corresponding changes in the electronic spectra (reduced intensity, blue-shifted Soret band, and new visible bands at long wavelengths) are known characteristics of porphyrin cation radicals, regardless of the identity of the metal and its oxidation state (see [52] and references therein). Additional and more specific information was provided by the EPR spectra, which are listed in Table 1. The pattern of three different *g* values, two around 4 and one at about 2, is only observed for iron porphyrins in which both the metal and the porphyrin are oxidized. Its interpretation requires strong ferromagnetic coupling between the two unpaired electrons of low-spin Fe(IV) with the single electron of the porphyrin cation radical, resulting in $S_{total}=3/2$ [13]. This is very different from that of iron(III) porphyrins, including *N*-oxide derivatives, which are sometimes formed under similar conditions [53]. In addition, all oxoiron(IV) porphyrins and iron(III) porphyrin cation radicals are EPR-silent. Still, the data in Table 1 show that the EPR spectra were not particularly sensitive to the identity of the axial ligand in the various **1**-X complexes. For this purpose, the ^1H NMR of the complexes, which are summarized in Table 2, were very useful. The general pattern of particular resonances was conserved in all complexes, but the exact chemical shifts were different for each **1**-X complex. The only obvious explanation for this phenomenon is

Scheme 4 Preparation of oxoiron(IV) tetramesitylporphyrin cation radical complexes by ozonolysis of the corresponding iron(III) porphyrins

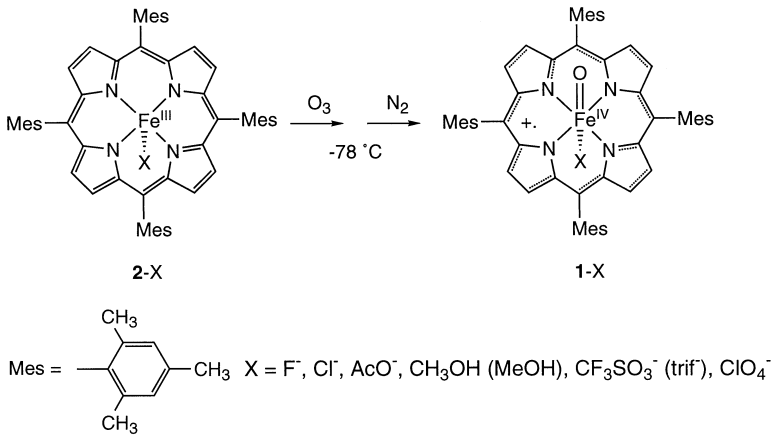

that the general structures of all complexes are identical, while the small differences are due to different axial ligands. The high-field chemical shifts (between -7 and -27 ppm) of the *pyrrole*-H resonances in all complexes also serves to rule out iron(III) porphyrin cation radicals, in which these resonances are at low field, as confirmed for the independently prepared $(TMP^{+}\cdot)Fe^{III}(ClO_4)_2$ and $(TMP^{+}\cdot)Fe^{III}(Cl)(SbCl_6)$ complexes, respectively. The lack of a reflection plane through the porphyrin ring is apparent from the observation of separate signals for the two *ortho*-CH_3 groups of each of the mesityl groups. This means that the two axial positions of the metal ion are occupied by different ligands: the original ligand of **2**-X and most probably an oxo ligand provided by the oxidant, ozone. The presence of the oxo ligand in the **1**-X complexes was proven by the previously reported RR measurements of the complexes, which are summarized in Table 4 [43]. Only one band, in the region of 801–835 cm^{-1}, was sensitive to ^{18}O vs ^{16}O substitution, with isotopic shifts of 34–36 cm^{-1}, which agrees closely with the calculated shift of 35.2 cm^{-1}. In conclusion, the combination of UV-vis, EPR, NMR, and RR clearly revealed that all **1**-X complexes have in common an iron(IV) metal, coordinated to a porphyrin cation radical in its equatorial plane and to an oxo ligand in one axial bond. The only reasonable explanation for the observed differences between the various **1**-X complexes is that the other axial position, *trans* to the oxoiron(IV) bond, is occupied by the original axial ligand in **2**-X.

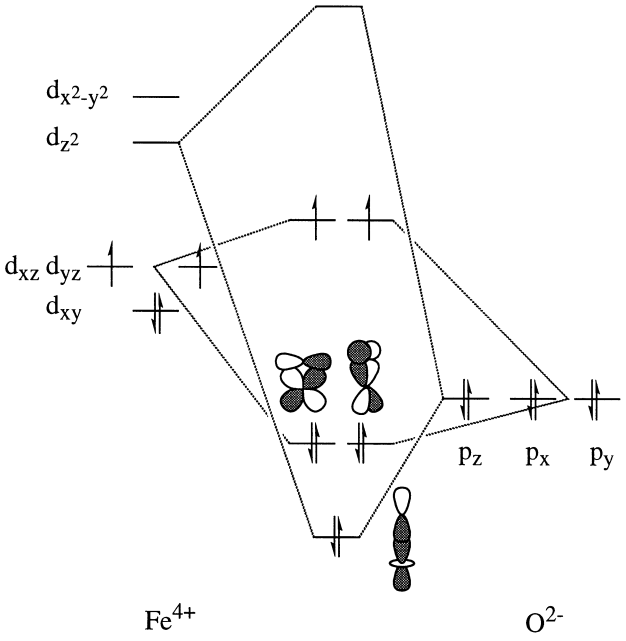

Fig. 2 Correlation diagram of the oxoiron(IV) bond, with emphasis on the 2c-2e σ-bond (p_z-d_{z^2}) and the pair of 2c-3e π-bonds (p_x-d_{xz} and p_y-d_{yz}) which together provide a bond order of 2

The effect of the axial ligands on the oxoiron(IV) bond strength in the **1**-X complexes

Of the various spectroscopic methods by which the **1**-X complexes were examined, the only relatively direct measurement for the effect of the axial ligands on the Fe=O bond strength comes from the RR $\nu_{Fe=O}$ frequencies. The results in Table 4 clearly show that the **1**-X complexes can be divided into two groups which differ in the value of their $\nu_{Fe=O}$ frequency by about 30 cm^{-1}, while within each group the values are almost identical. We thus conclude that, with F^-, Cl^-, and mCB^- (3-chlorobenzoate) as axial ligands ($\nu_{Fe=O}$ = 801–806 cm^{-1}), the oxoiron(IV) bond is weaker than with $HOCH_3$, $trif^-$, and ClO_4^-, ($\nu_{Fe=O}$ = 831–835 cm^{-1}). An obvious difference between the two groups is that the first group includes the ligands which are expected to be stronger electron donors than those of the second group. The bond-weakening effect of *trans*-donor ligands is readily accounted for by simple MO considerations of the Fe=O moiety, shown in Fig. 2. The bond order of 2 of the d^4 low-spin Fe(IV) ion – $(d_{xy})^2(d_{xz})^1(d_{yz})^1$ – with O^{2-} is achieved by one two-electron d_{z^2}-p_z σ-bond and two three-electron π-bonds, d_{xz}-p_x and d_{yz}-p_y. Accordingly, donation of both σ and π electrons by *trans* ligands are expected to destabilize the Fe=O bond. It is, however, surprising that these effects are not reflected in differ-

Table 4 Selected Resonance Raman (cm^{-1}, in CH_2Cl_2 at $-60\,°C$ [43]) and NMR (δ, ppm) data for the various oxoiron(IV) tetramesitylporphyrin cation radical complexes **1**-X and the iron(III) tetramesitylporphyrin complexes **2**-X

X in **1**-X and **2**-X	F^-	Cl^-	AcO^-	MeOH	$trif^-$	ClO_4^-
$\nu_{Fe=O}$ in **1**-X	801	801	806[a]	831	834	835
ν_2 in **1**-X	1530	1531	1533[a]	1517	1520	1515
ν_2 in **2**-X	1555	1555	1555[a]	[b]	1654	1567
$\Delta\nu_2$[c]	25	24	22[a]	[b]	44	52
pyr-H in **1**-X[d]	−13.0	− 6.7	− 8.3	−26.7	−26.2	−26.9
pyr-H in **2**-X[e]	81.5	80.3	79.6	[b]	52.6	29.2

[a] Data for **1**-mCB
[b] **2**-MeOH cannot be prepared
[c] ν_2(**2**-X) − ν_2(**1**-X)
[d] In CD_2Cl_2 at $-80\,°C$
[e] In C_6D_6 at RT

entiation within the two groups, for example between F^- and Cl^-.

A plausible explanation for this dilemma relies on the two other ligand-sensitive spectroscopic features of the **1**-X complexes, the RR ν_2 mode and the ^1H NMR chemical shifts of the β-pyrrole hydrogens. Examination of Table 4 shows that the above-mentioned pattern is conserved here too, as the ν_2 frequencies are about 1530 cm^{-1} for X = F^-, Cl^-, mCB^-, but $\nu_2 \leq 1520\ cm^{-1}$ for X = $HOCH_3$, $trif^-$, ClO_4^-. Similarly, the chemical shifts of the first three complexes are -9.85 ± 3.15 ppm, but less than −26 ppm for the three others (Table 2). It is very well known that the ν_2 frequency reflects the $C_{\beta\text{-pyrrole}}$-$C_{\beta\text{-pyrrole}}$ bond strength and is highly sensitive to the symmetry of the porphyrin's HOMO, which is a_{2u} for metal complexes of TMP under D_{4h} symmetry [52]. The highest possible symmetry for both the **1**-X and **2**-X complexes is C_{4v}, under which both the metal-axial ligand σ-bond and the porphyrin's HOMO are of a_1 symmetry. Donation of σ-electrons by axial ligands is expected to weaken the fully occupied $C_{\beta\text{-pyrrole}}$-$C_{\beta\text{-pyrrole}}$ bonds in **2**-X, but to increase their strength in **1**-X in which the porphyrin orbital is only singly occupied. These effects are very nicely reflected in the RR spectra of the present series of complexes. A monotonic shift to higher frequencies of ν_2 is observed in the **2**-X complexes – 1555, 1555, 1564, and 1567 cm^{-1} for X = F^-, Cl^-, $trif^-$, and ClO_4^-, respectively – which is in contrast to shifts to lower frequencies of ν_2 – 1530, 1531, 1520, and 1515 cm^{-1} – for the same axial ligands in the **1**-X complexes. We may thus conclude from the RR results, which are presented in the fourth row of Table 4 as the difference between the ν_2 frequencies in the **1**-X and **2**-X complex of each axial ligand, that the σ-donating ability is $F^- \approx Cl^- \approx mCB^- > trif^- > ClO_4^-$. The same conclusion is reached by analysis of the NMR spectra of the (TMP)Fe(X) complexes. The very large isotropic shift of *pyrrole*-Hs in high-spin iron(III) porphyrins is known to be due to strong σ-interactions between the nitrogen's lone pairs and the metal's d_σ orbitals [54]. As the axial ligand becomes weaker, the d_{z^2} orbital is stabilized at the expense of the $d_{x^2-y^2}$ orbital, whose energy is raised. Eventually, this results in $S = 5/2$, $S = 3/2$ spin-admixed structures and finally in intermediate-spin complexes [55]. In the latter, the *pyrrole*-H chemical shift is about −30 ppm. Thus, the current data for the *pyrrole*-H chemical shifts – 81.5, 80.3, 79.6, 52.6, 29.6 ppm for F^-, Cl^-, AcO^-, $trif^-$, ClO_4^-, respectively – reflects the σ-donor strength of the ligands in that order, in complete agreement with the RR results.

An indication of the π-donor ability of the ligands can be acquired from the chemical shifts of the *pyrrole*-Hs in the NMR spectra of the **1**-X complexes [54, 56]. To the best of our knowledge, the NMR of oxoiron(IV) porphyrin cation radicals was never analyzed in terms of the origin of the isotropic shifts. But, the upfield shifts suggest a π-spin transfer from the porphyrin's 3e (filled) to the metal's $d\pi$ orbitals, as in the isoelectronic (but high-spin) d^4 (POR)Mn(III)-X complexes [54]. The changes in the contact shifts as a function of axial ligands are described as reflecting competition between X and porphyrin as electron donors to the metal: as the π-donor strength of X increases, the extent of porphyrin → metal donation decreases, resulting in a decreased shift of the *pyrrole*-Hs. Thus, the *β-pyrrole*-CH chemical shifts for X = F^-, Cl^-, AcO^-, ClO_4^- are −20.8, −21.8, −22.3, −35.5 ppm, respectively, in (TMP)Mn-X [47] and −19.7, −22.3, −21.8, −36.0 ppm, respectively, in (TPP)Mn-X complexes [57]. Similarly, the results collected in Table 2 support a relative π-donor strength series in the **1**-X complexes of: $Cl^- > AcO^- > F^- \gg trif^- > MeOH > ClO_4^-$. By taking into account this π-donor strength together with the σ-donor strength order of $F^- > Cl^- > AcO^-$ (mCB^-) $\gg trif^- > ClO_4^-$, the effects of the axial ligands on the Fe=O bond strength are quite well rationalized. The first three ligands display an opposite trend in their relative σ- and π-donor strengths, which, together with the small differences within the series, are responsible for the almost identical Fe=O bond strength. On the other hand, the $trif^-$ and ClO_4^- ligands are much weaker σ- and π-donors, and accordingly the oxoiron(IV) bond in their complexes is significantly stronger.

These considerations enable the first step in the construction of a reaction profile for the reactions of the **1**-X complexes with olefins, which is their relative ground state energy. Considering only the strength of the oxoiron(IV) bond, the relative order is **1**-F = **1**-Cl > **1**-OAc ≫ **1**-$HOCH_3$ > **1**-trif ≈ **1**-$OClO_3$.

No correlation between oxoiron(IV) bond strength and reactivity

The last step in the epoxidation of olefins under catalysis by cytochrome P-450 or synthetic iron porphyrins is usually considered to be oxygen atom transfer from oxoiron(IV) porphyrin cation radical to alkene, producing iron(III) porphyrin and epoxide. For a one-step mechanism, a correlation between the oxoiron(IV) bond strength of the catalyst and its reactivity is expected. Accordingly, we have examined the rate of epoxide formation in the reactions of the various **1**-X complexes with one representative olefin, styrene. Reactions were initiated by adding excess olefin to dry ice/acetone cooled solutions of the particular preformed **1**-X complex, after removal of excess ozone by nitrogen (Scheme 5). The advantage of this procedure was that, unlike the situation under catalytic conditions, there was no doubt about the identity of the reactant. In all cases except for **1**-$OClO_3$, where no organic products were formed under these conditions, the sole organic product was styrene oxide. In addition, excellent pseudo-first-order kinetic profiles were obtained (Fig. 1, inset), which enabled the elucidation of the second-order rate constants for these stoichiometric oxidation reactions (Fig. 1 and Table 3). The results show that the effect of the axial ligands is quite pronounced. Thus, the rate constant of **1**-F is 15 times larger than that of **1**-trif, and in the reaction with **1**-ClO_4 no organic product was formed. However, there is no correlation between the reactivity and the spectroscopic features of the complexes. While the **1**-F and **1**-Cl complexes have identical Fe=O stretching frequencies, the reaction of **1**-F with styrene is almost 5 times faster than that of **1**-Cl. Furthermore, **1**-$HOCH_3$ ($\nu_{Fe=O}=831$ cm^{-1}) reacts with not only more than 4 times faster than **1**-trif ($\nu_{Fe=O}=834$ cm^{-1}), but even faster than **1**-Cl, whose $\nu_{Fe=O}$ is 801 cm^{-1}. The necessary conclusion is that there is no correlation between the *thermodynamic* effect of the axial ligands, as reflected in the RR and NMR data of the **1**-X complexes, and their *kinetic* effect as displayed by the rate of reaction with styrene. In classical terminology [58], the thermodynamic and kinetic effects of the ligands on the oxoiron(IV) moiety are the *trans* influence and the *trans* effect, respectively. Similarly, the absence of correlation between thermodynamic and kinetic data of the reactants presents a violation of the concept of linear free energy relationships (LFER) [59].

The most reasonable rationale for such a phenomenon is that the reaction under study consists of several elementary steps, the first not being rate limiting. In such cases, the *trans* influence on the intermediate can be very different from that in the reactant, resulting in an apparent mismatch between the thermodynamic and kinetic effects of the ligands. This proposal is in line with the very strong evidence for a multistep mechanism in the reactions of oxoiron(IV) porphyrin cation radicals with olefins [34–42]. In particular, complexes which contain both reactants in the form of either charge transfer, electron transfer, metallacycle, or radical species are frequently proposed as intermediates in these reactions. In order to construct the full reaction profile of the reaction and to understand the seemingly different effects of the iron's axial ligand on the various elementary steps, we decided to acquire more detailed information about the electronic structure of the proposed reaction intermediate.

Spectroscopic characterization of an intermediate in the reaction of **1**-ClO_4 with olefins

In the previous section, it was mentioned that in the reaction of **1**-ClO_4 with styrene no organic products were formed. There are at least three possible reasons for this observation: (a) **1**-ClO_4 decomposed before the addition of the olefin, (b) **1**-ClO_4 did not react with the olefin, i.e. the reaction mixture still contains the original components, or (c) **1**-ClO_4 decomposed in an olefin-dependent fashion, but without forming detectable organic products. The first possibility can easily be ruled out, as all the earlier-mentioned spectroscopic measurements of aged and fresh samples samples were identical. It was also clear that at least the porphyrin remained oxidized after addition of the olefins, since the characteristic green color of porphyrin cation radicals did not disappear. In fact, an increase in its intensity was noticed, similar to that obtained in the studies of Groves and Watanabe [41]. In order to gain more insight into the behavior of the oxidized catalyst, the reaction of **1**-ClO_4 with styrene was examined by spectroscopic methods.

Addition of styrene-d_8 to a preformed and pre-examined (Fig. 3a) solution of **1**-ClO_4 in CD_2Cl_2 at

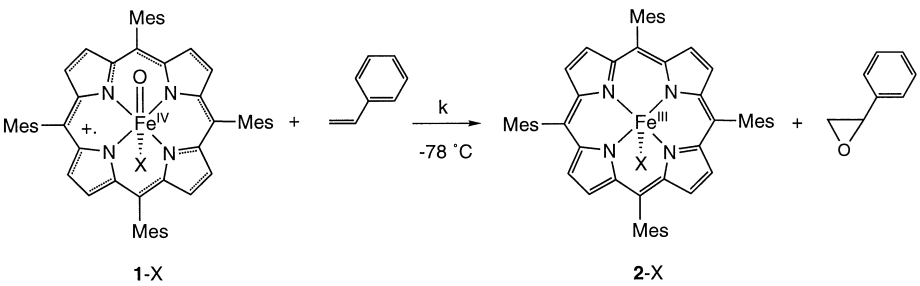

Scheme 5 Reaction of the oxoiron(IV) tetramesitylporphyrin cation radical complexes with styrene

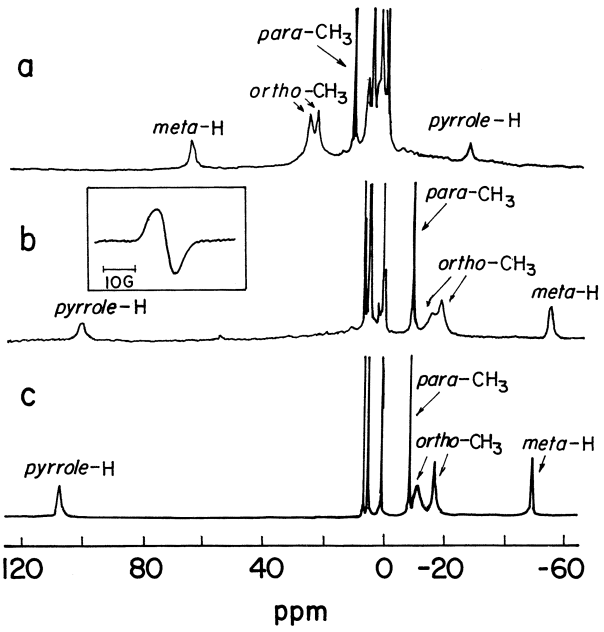

Fig. 3 ^{1}H NMR spectra in CD_2Cl_2 at −80 °C of **a** $(TMP^+\cdot)Fe(IV)(O)(ClO_4)$, **1**-$ClO_4$, **b** **3**-$ClO_4$, obtained by addition of styrene-d_8 to the solution of trace **a** (*Inset:* ESR spectrum of the same solution), and **c** independently prepared $(TMP^+\cdot)Fe(III)(Cl)(SbCl_6)$

−80 °C resulted in a new spectrum (Fig. 3b), very different from that of the reactant. The spectrum was also very different from that of the expected final product (TMP)Fe(III)(ClO_4), **2**-ClO_4 [δ (ppm) 11.1 (*m*-H), 4.5 (*p*-CH_3), 3.9 (*o*-CH_3), −26 (*pyr*-H) at −80 °C]. Since the green color of the sample strongly indicated the existence of a porphyrin radical, we have also independently prepared NMR solutions of $(TMP^+\cdot)Fe(III)(ClO_4)_2$ (δ (ppm) 97 (*m*-H), 43.6 (*o*-CH_3), 27.4 (*p*-CH_3), −26 (*pyr*-H) at −80 °C) and $(TMP^+\cdot)Fe(III)(Cl)(SbCl_6)$, whose spectrum is presented in trace c of Fig. 3. Examination of the traces of Fig. 3 clearly shows that the spectrum of the complex formed by addition of styrene to **1**-ClO_4 is different from all other traces except that of $(TMP^+\cdot)Fe(III)(Cl)(SbCl_6)$, to which it is quite similar. The assignments of the resonances in trace b to particular protons was achieved by taking into account relative integration, relative linewidths, and experiments in which pyrrole-deuterated **2**-ClO_4 served as starting material [60]. In particular, the two most shielded resonances, at +100 and −55 ppm with identical integration, were assigned as β-pyrrole and *m*-aryl protons, respectively, by the deuterated complexes. The three other resonances at −9, −14, and −18 ppm were identified as CH_3 groups of the mesityl rings by the 3:2 integration of each of them to either the pyrrole or *m*-H protons. Finally, the relatively small isotropic shift and linewidth of the signal at −9 ppm leads to its assignment as the *p*-CH_3 groups, and accordingly the two remaining relatively broad resonances must be due to two sets of different *o*-CH_3 groups. Based on these assignments and the similarity to $(TMP^+\cdot)Fe(III)(Cl)(SbCl_6)$, we conclude that the complex formed by the reaction with styrene (complex **3**-ClO_4) is also an iron(III) porphyrin cation radical with two very different axial ligands. A plausible partial structure for complex **3**-ClO_4 is $[(TMP^+\cdot)Fe(III)(O)(ClO_4)]^-$, formed by one-electron reduction of the oxoiron(IV) moiety of **1**-ClO_4, $[(TMP^+\cdot)Fe(IV)(O)(ClO_4)]$ (Scheme 6). Supporting evidence for the quite unusual structure of **3**-ClO_4 is provided by the electrochemical oxidation of (TMP)Fe(III)OH to (TMP)Fe(IV)O, in which $(TMP^+\cdot)Fe(III)(OH)(ClO_4)$ (a protonated form of $[(TMP^+\cdot)Fe(III)(O)(ClO_4)]^-$) is formed as a transient [45, 61]. This proposal accounts for all the spectroscopic features of **3**-ClO_4: the $(TMP^+\cdot)$ part being responsible for the green color, the singly occupied $d_{x^2-y^2}$ orbital of Fe(III) for the large isotropic shift to low field of the β-pyrrole hydrogens [53], and the two different axial ligands for the unequivalence of the *o*-CH_3 chemical shifts (the identity of the axial ligands is further discussed in the next section).

The complete structure of complex **3**-ClO_4 must also include a cation, which, based on the redox reaction that occurred by addition of styrene to **1**-ClO_4, is expected to be $[styrene]^+\cdot$. To test this hypothesis, a quartz NMR tube of **3**-ClO_4 in CD_2Cl_2 was examined by ESR at −80 °C (above the freezing temperature of the solvent). The resulting ESR spectrum is displayed in the inset of Fig. 3b. The strong signal at $g \approx 2$ must be due to an organic radical, since all iron porphyrins are "ESR-silent" in liquid solutions, regardless of oxidation state of the porphyrin or the iron. Further details could not be obtained from the ESR spectrum of **3**-ClO_4 since no hyperfine structure was observed, probably due to the closeness of the organic radical to the other paramagnetic centers, the porphyrin radical and the metal. We thus propose that the full structure of complex **3**-ClO_4 is either an ion pair $[(TMP^+\cdot)Fe(III)(O)(ClO_4)]^-[styrene]^+\cdot$ or $[(TMP^+\cdot)Fe(III)(OCH_2\text{-}CH\cdot\text{-}C_6H_5)(ClO_4)]$, in which a σ bond exists between the oxygen and the terminal methylene of styrene, leaving behind a benzylic radical (the "σ-bound form" in Scheme 6). Both structures are fully consistent with all the results presented so far.

Is complex **3** a true reaction intermediate?

This crucial question was addressed by investigating the reactivity of the preformed intermediate complex **3**-ClO_4. An NMR solution of **3**-ClO_4 – stable for days at −78 °C – was gradually warmed until decomposition was observed. This occurred at −30 °C, where a clean conversion to **2**-ClO_4 took place. After full formation of **2**-ClO_4, the reaction mixture was quenched and examined for organic products by GC analysis, which revealed that styrene oxide and phenylacetaldehyde were found in 17 and 5%, respectively (up to 65% yields of these products were obtained by warming the solutions

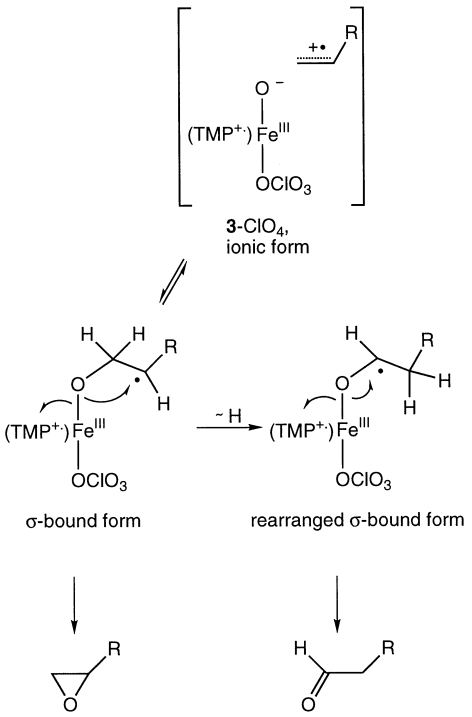

Scheme 6 The proposed equilibrium between the ionic and covalent forms of intermediate **3**-ClO_4

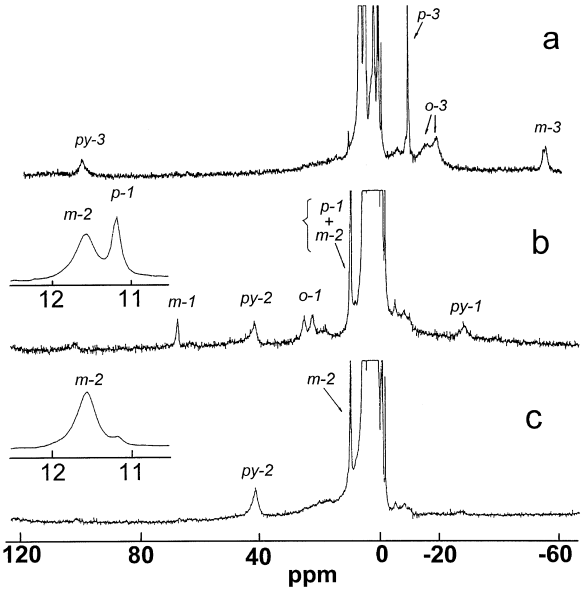

Fig. 4 ^1H NMR spectra in CD_2Cl_2 at −80 °C of **a** the reaction intermediate **3**-ClO_4, obtained by addition of styrene to a solution of **1**-ClO_4, **b** the same solution as in trace **a**, 5 min after addition of CD_3OD (5%, v/v), and **c** the same solution as in traces **a** and **b**, 1 h after addition of CD_3OD. *py* = *pyrrole*-H, *p* = *para*-CH_3, *m* = *meta*-H, *o* = *ortho*-CH_3. 3, 1, and 2 stand for complexes **3**-ClO_4, **1**-MeOD, and $[(TMP)Fe(III)(MeOD)_2]^+$, respectively. For identification of the last two complexes, see text

to room temperature immediately). This experiment provided evidence for several points: (a) Since a perchlorato ligand is present in both the reactant and the product, it must be preserved in complex **3**-ClO_4 also. (b) The oxygen atom transfer to the olefin requires that the second axial ligand in **3**-ClO_4 contains oxygen. (c) The oxidation ability is conserved in **3**-ClO_4, which proves that complex **3** is a true reaction intermediate which leads to oxygenation. A different experiment was performed for elucidation of the role of the perchlorato ligand in the apparent stabilization of complex **3**-ClO_4, i.e. by adding CD_3OD to an NMR tube of **3**-ClO_4 at −80 °C. Since it is well known that CD_3OD will replace any axial ligand *trans* to the oxoiron(IV) bond in **1**-X [21–23], we expected a similar ligand exchange for complex **3**-ClO_4 also. As shown in Fig. 4b, the NMR spectrum recorded immediately after the addition of CD_3OD contained no more **3**-ClO_4 (compare with Fig. 4a). Instead, an approximately equimolar mixture of **1**-CD_3OD [21–23] and $[(TMP)Fe(III)(CD_3OD)_2]^+$ (identified by its independent preparation from (TMP)Fe(III)(ClO_4) in a 5% CD_3OD/CD_2Cl_2 solution) was formed. The constitution of this mixture changed gradually in the course of 1 h, after which the spectrum was almost exclusively that of $[(TMP)Fe(III)(CD_3OD)_2]^+$ (Fig. 4c). At the end of this route, 24% styrene oxide and 20% phenylacetaldehyde were identified by GC. Again, this experiment clearly shows that complex **3**-ClO_4 is on the reaction pathway from oxoiron(IV) porphyrin cation radicals and olefins to iron(III) porphyrin and oxygenated alkene. The reversibility of the process leading from **1** to **3**-ClO_4 – also previously noted by Groves and Watanabe in a different set of experiments [41] – supports the assignment of **3**-ClO_4 as an ionic rather than a covalent complex.

Similar spectroscopic investigations were also performed with **1**-Cl and **1**-trif at −80 °C. In the reaction of **1**-Cl with styrene, a smooth and clean conversion to **2**-Cl (NMR) and styrene oxide (GC) was observed without formation of any other porphyrin intermediate. But, with **1**-trif as oxidant, three different complexes were observed in the reaction mixture by NMR: **1**-trif (the reactant), **2**-trif (the product), and a complex with spectroscopic features of **3**-ClO_4 (**3**-trif). Both the signals due to **2**-trif and **3**-trif disappeared with time in favor of **2**-trif, and styrene oxide was identified by GC as the sole organic product. These results indicate that similar intermediates are most probably on the reaction pathway for all **1**-X complexes: stable and readily observable for X = ClO_4, metastable and in steady-state concentration for X = trif, and at much higher-energy, possibly transition states, for X = Cl. This provides additional information for the desired construction of the full reaction profile.

An additional important observation was that only in the reactions with **1**-ClO_4, where the intermediate complex **3**-ClO_4 had a very long lifetime, large amounts of phenylacetaldehyde were formed. It was already proven that this product is not a result of rearrangement of styrene oxide, but a primary product (see [62]

and references therein). We have also noticed in the present studies that different product ratios were obtained when solutions of **3**-ClO_4 were warmed to −30 °C or directly to room temperature. To account for these results, we suggest an equilibrium between the ionic form suggested for **3**-ClO_4 and a structure in which a covalent bond is formed between the Fe-O^- moiety and the olefin radical cation. As shown in Scheme 6, only the covalent form allows isomerization which will lead to phenylacetaldehyde. On the other hand, the earlier-mentioned reversibility of the transformation of **1**-ClO_4 to **3**-ClO_4 proceeds most probably through the ionic form. Thus, both the ionic and the σ-bound forms of Scheme 6 are required to account for all results.

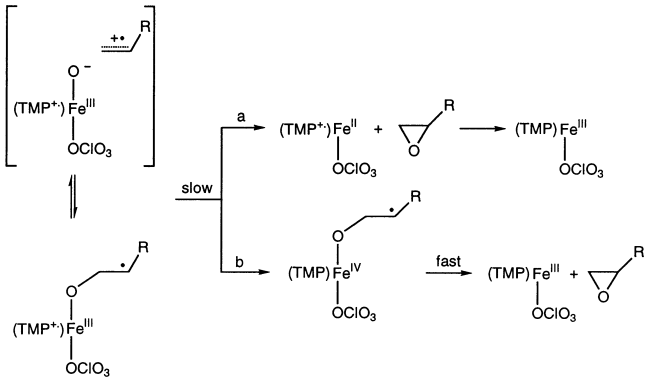

Scheme 7 Reaction pathways for decomposition of the intermediate complex **3**-X to products

How do axial ligands affect the decomposition of the reaction intermediate to final products?

Up to now we have been concerned with the relative energies of the **1**-X complexes and the **3**-X reaction intermediates. It became quite clear that the axial ligands have a pronounced effect on the stability and/or the reactivity of **3**-X, which is related to the rate of epoxide formation. Thus, **3**-ClO_4 is stabilized to such a large extent that no epoxide is formed, **3**-trif is less stable and decomposes to products slowly at −80 °C, and with the other ligands the reaction intermediate is too unstable to be observed and the rate of epoxide formation is much larger. These observations lead to the conclusion that the rate-limiting step in the overall transformation of **1**-X and olefin to **2**-X and epoxide is the decomposition of the **3**-X intermediate. Our proposal for the effect of axial ligands on the transformation of **3**-X to **2**-X and epoxide is shown in Scheme 7. Since in **3**-X the iron is +3 and the porphyrin is still oxidized, direct formation of epoxide through route a will produce an implausible iron(II) porphyrin cation radical. A more reasonable pathway (b in Scheme 7) is prior intramolecular electron transfer from iron to porphyrin to produce an iron(IV) species which will release the epoxide accompanied by formation of **2**-X, an iron(III) porphyrin. The kinetic results suggest that the effect of the axial ligands in the **3**-X intermediates is on the intramolecular iron to porphyrin electron transfer. This proposal gains support from the very well-known phenomenon of ligand-dependent preference for the oxidation site in one-electron-oxidized iron(III) and manganese(III) porphyrins. Either the porphyrin or the metal are oxidized, resulting in $(POR^{+}\cdot)M(III)(X)_2$ and $(POR)M(IV)(X)_2$, respectively. In Table 5, various examples from the literature and a few of our own are summarized to emphasize this point. Generally, the preference for metal oxidation is larger for manganese than for iron due to the d^3 configuration of Mn(IV). Still, the effect of the ligands on the oxidation site in the (POR)M(X)(Y) complexes is very clear. Starting from the bottom of Table 5, it is apparent that in the presence of at least one very weak ligand, i.e. $X = Y = ClO_4^-$ and $X = Cl^-$, $Y = SbCl_6^-$, the porphyrin is oxidized for both Fe and Mn. The differences between ClO_4^-, $trif^-$ and Cl^- are nicely reflected in the Mn porphyrin series: for $X = Y = ClO_4^-$ the porphyrin is oxidized, for $X = Y = trif^-$ the $(TPP^{+}\cdot)Mn(III)(trif)_2$ and $(TPP)Mn(IV)(trif)_2$ structures are about the same energy [63], while for $X = Y = Cl^-$ the metal is oxidized [47]. Finally, for $X = Y = CH_3O^-$ and $X = Y = F^-$, the oxidation site is the metal even for iron [64, 65]. Based on

Table 5 One-electron oxidation products of various Fe(III) and Mn(III) porphyrins

Axial ligands; X, Y	Iron			Manganese		
	Porphyrin oxidation	Metal oxidation	References	Porphyrin oxidation	Metal oxidation	References
F^-, F^-		$(TPP)Fe(F)_2$	[64]			no data
CH_3O^-, CH_3O^-		$(TMP)Fe(OCH_3)_2$	[50]		$(TPP)Mn(OCH_3)_2$	[63]
Cl^-, Cl^-			no data		$(TMP)Mn(Cl)_2$	[47]
$trif^-$, $trif^-$			no data	$(TPP^{+}\cdot)Mn(trif)_2$	$(TPP)Mn(trif)_2$	[62]
AcO^-, AcO^-	$(TMP^{+}\cdot)Fe(OAc)_2$		this work			no data
Cl^-, $SbCl_6^-$	$(TMP^{+}\cdot)Fe(Cl)(SbCl_6)$		this work	$(TMP^{+}\cdot)Mn(Cl)(SbCl_6)$		[47]
ClO_4^-, ClO_4^-	$(TMP^{+}\cdot)Fe(ClO_4)_2$		[50], [45], and this work	$(TMP^{+}\cdot)Mn(ClO_4)_2$		[47]

this data we thus suggest that the ability to trap **3**-ClO_4 and to observe **3**-trif as a metastable intermediate is due to the relatively large kinetic barrier for intramolecular electron transfer required to accomplish the final pathway to products (pathway b in Scheme 7). The data in Table 5 strongly support the proposal that this barrier is decreased in the order of $F^- < Cl^- < AcO^- < trif^- < ClO_4^-$, which is exactly the order of reactivity of the **1**-X complexes. In conclusion, we propose that the step from the **3**-X complexes to final products is fully rate limiting for $X = ClO_4^-$, and at least partially so for the other complexes. As the first step in the reaction of the **1**-X complexes with olefin is not rate limiting, this explains the apparent discrepancy between the earlier-mentioned thermodynamic and kinetic effects of the axial ligands.

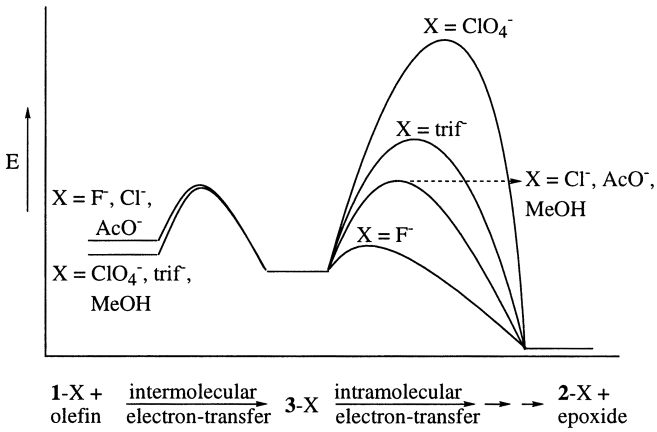

Scheme 8 Reaction profile for the reaction of oxoiron(IV) porphyrin cation radical complexes coordinated by different axial ligands (**1**-X) with olefins to produce iron(III) porphyrin (**2**-X) and epoxide via intermediate electron transfer complexes (**3**-X)

The full reaction profile for reaction of oxoiron(IV) porphyrin radicals with olefins

The combination of all the results enables the construction of a full reaction profile for the reaction of the **1**-X complexes with olefins, shown in Scheme 8. The **1**-F, **1**-Cl, and **1**-OAc complexes were drawn at slightly higher energy than **1**-ClO_4, **1**-trif, and **1**-MeOH to reflect the somewhat weaker Fe=O bonds of the former. We propose that the initial step is identical for all complexes, i.e. electron transfer from olefin to metal. However, this step cannot be rate limiting because of the absence of correlation between the kinetic results and the Fe=O stretches. The difference is also only about 30 cm^{-1}, less than 0.1 kcal/mole, much too small to account for the differences in the reactivities of the **1**-X complexes. The reactions of **1**-trif and **1**-ClO_4 were shown to proceed through an observable electron transfer intermediate, whose further transformation to the final product is rate limiting, and much more facile for **3**-trif than for **3**-ClO_4. The trapping of **3**-ClO_4 enforces the very large activation energy for its decomposition drawn in the Scheme. For **3**-MeOH, which was prepared by addition of MeOH to **3**-ClO_4, its decomposition to about equimolar amounts of products and reactant (**1**-MeOH) indicates that the activation energy of the second step is only slightly lower than that of the reversal of the first step. The situation is probably similar for **1**-OAc and **1**-Cl, which react at about the same rate as **1**-MeOH. Thus, the major effect of the axial ligands is on the step in which the **3**-X complexes rearrange by intramolecular electron transfer from the iron(III) porphyrin radical structure to iron(IV) porphyrin. The preference for the iron(IV) porphyrin state in the order $X = F^- > Cl^- > trif^- > ClO_4^-$ was elucidated from similar phenomena in one-electron oxidized iron(III) and manganese(III) porphyrins and was found to be identical to the reactivity order of the present series. Finally, the very high reactivity of the **1**-F complex indicates that the electron transfer from olefin to metal is already accompanied by a shift of the reduction site from iron to the porphyrin radical. This proposal is supported by the finding of Goff et al. for oxidation of (TPP)Fe-F in the presence of fluoride anions. Not only is the oxidation product $(TPP)Fe^{IV}(F)_2$ and not $(TPP^{+}\cdot)Fe^{III}(F)_2$, but the oxidation potential is much lower than for porphyrin oxidation [65].

Further implications of the proposed reaction profile

In the previous sections we have shown that the σ-bound form of intermediate **3**-X readily accounts for formation of aldehyde (Scheme 6), the common by-product in iron(III)-porphyrin-catalyzed epoxidations. However, such a radical intermediate seems contradictory to the well-known high stereo-retention in catalytic epoxidation of *cis* olefins by both P-450 and the model complexes [66, 67]. For a long-lived radical intermediate, rotation of the substituent α to the radical will necessarily lead to loss of stereochemistry, i.e. production of significant amounts of *trans* epoxides from *cis* olefins. This apparent contradiction was resolved by the temperature-dependent investigation of the (TMP) Fe-X (X = Cl, F, ClO_4) catalyzed epoxidation of *cis*-β-methylstyrene by iodosylbenzene. In accord with other reports [62, 68], for the reactions performed at either room temperature or 0 °C, the stereo-retention was very large indeed (>96% *cis* epoxide), but at −78 °C the major product was the *trans* epoxide. This was true not only for the catalytic reaction (*trans*/*cis* = 4.5), but also for stoichiometric reactions performed by adding *cis*-β-methylstyrene to preformed solutions of **1**-X by either ozone or *m*-CPBA, in which the *trans/cis* ratios were in the range 1.2–2.0. Our conclusion is that at high temperatures the release of product is faster than isomerization, but that at low temperatures the lifetime of the **3**-X intermediate is long enough as to allow for isomerization. Interestingly, we have recently noticed an intriguing phenomenon in en-

antioselective epoxidation of styrene in a chiral iron-(III)-porphyrin-catalyzed process [69], which is readily understandable by the same arguments. The enantiomeric excess (ee) of the styrene oxide product increased by gradually lowering the reaction temperature to −20 °C, but at still lower temperatures the ee decreased significantly. Again, our interpretation is that the increased lifetime of the reaction intermediate at low temperatures allows for rotation, which in this case leads to racemic products. Similar conclusions were reached for enantioselective epoxidation of styrene by chiral manganese salen complexes [70].

Finally, we wish to address the relevance of the present system to the cysteinate-ligated P-450 enzymes. Since even iron(III) and thiolate are a redox couple, thiolate complexes cannot be utilized in studies of simple compound I model complexes (see however the elegant studies of Higuchi and Hirobe [71] and references therein). Still, the conclusions of our studies are very much supportive of the recent proposals regarding the involvement of the thiolate ligand in providing an additional tautomer in the already existing redox tautomerism (between metal, oxygen, porphyrin, and protein) of compound I's ground state [14, 72, 73]. Our results emphasize the effect of axial ligands on the transformation of the iron(III) porphyrin radical intermediate (most stable with ClO_4^-) to iron(IV) porphyrin (most stable with F^-). As the electronic structures of the two species involved in this intramolecular electron transfer process could in principle be presented as resonance structures, an additional "resonance-structure", in which the unpaired electron is localized on the redox-active thiolate, will significantly reduce the *kinetic* barrier of iron(III) to porphyrin radical electron transfer. Finally, since the NMR features of the intermediate are indicative of high-spin iron(III), whereas iron(IV) porphyrins are invariably low-spin [45, 50], an additional role of the cysteinate could be the moderation of this spin state change.

Conclusions

The reaction mechanism of olefin epoxidation by model complexes of cytochrome P-450's compound I was investigated by elucidating the effect of a single variable – the axial ligand *trans* to the oxoiron(IV) bond – on the thermodynamic and kinetic properties. It was shown that the effect of the *trans* ligands on the oxoiron(IV) bond strengths is real, but too small to account for the widely different reactivities. All evidence points toward a multistep reaction mechanism which contains two important partially rate-limiting elementary steps: one-electron transfer from olefin to the Fe=O moiety and intramolecular electron transfer from iron to porphyrin radical. The large effect of the axial ligands is on the transformation of $[(TMP^{+}\cdot)Fe(III)(O)(X)]^-$ to [(TMP)Fe(IV)(O)(X)]. The combination of all results allowed the construction of a full reaction profile for the reactions of the synthetic oxoiron(IV) porphyrin radical complexes with olefins, including a proposal for the role of the cysteinate ligand in cytochrome P-450 enzymes.

Acknowledgement This research was supported by grant No. 94-00373 from the United States-Israel Binational Science Foundation (BSF), Jerusalem, Israel.

References

1. Collman JP, Gagne RR, Reed CA, Halbert TR, Lang G, Robinson WT (1975)J Am Chem Soc 97:1427–1439
2. Morgan B, Dolphin D (1987) Structure and Bonding 64:115–203
3. Ortiz de Montellano PR (ed) (1986) Cytochrome P-450, structure, mechanism, and biochemistry. Plenum, New York London
4. Andersson LA, Dawson JH (1990) Structure and Bonding 74:1–40
5. Mansuy D (1994) Pure Appl Chem 66:737–744
6. Meunier B (1994) In: Montanari F, Casella L (eds) Metalloporphyrins catalyzed oxidations. Kluwer, Dordrecht Boston London, pp 1–47
7. Collman JP, Zhang X, Lee VJ, Uffelman E, Brauman JI (1993) Science 261:1404–1411
8. Groves JT, Han Y (1995) In: Ortiz de Montellano PR (ed) Cytochrome P-450, structure, mechanism, and biochemistry (2nd edn). Plenum, New York London, Chapter 1
9. Egawa T, Shimada H, Ishimura Y (1994) Biochem Biophys Res Commun 201:1464–1469
10. Edwards SL, Xuong N-H, Hamlin RC, Kraut J (1987) Biochemistry 26:1503–1511
11. Schultz CE, Rutter R, Sage JT, Debrunner P, Hager LP (1984) Biochemistry 23:4743–4754
12. Rutter R, Hager LP, Dhonau H, Hendrich M, Valentine M, Debrunner P (1984) Biochemistry 23:6809–6816
13. Trautwein AX, Bill E, Bominaar EL, Winkler H (1991) Structure and Bonding 78:1–95
14. Weiss R, Mandon D, Wolter T, Trautwein AX, Müther M, Bill E, Gold A, Jayaraj K, Terner J (1996) JBIC 1:377–383
15. Watanabe Y, Groves JT (1992) In: Sigman DS (ed) Mechanisms of catalysis. (The enzymes, vol 20) Academic, San Diego London, pp 406–452
16. Groves JT, Haushalter RC, Nakamura M, Nemo TE, Evans BJ (1981) J Am Chem Soc 103:2884–2886
17. Bill E, Ding XQ, Bominaar EL,Trautwein AX, Winkler H, Mandon D, Weiss R, Gold A, Jayaraj K, Hatfield WE, Kirk ML (1990) Eur J Biochem 188:665–672
18. Hashimoto S, Tatsuno Y, Kitagawa T (1987) J Am Chem Soc 109:8096–8097
19. Kincaid JR, Schneider AJ, Paeng KJ (1989) J Am Chem Soc 111:735–737
20. Penner-Hahn JE, McMurry TJ, Renner MW, Latos-Grazynski L, Eble KS, Davis IM, Balch AL, Groves JT, Dawson JH, Hodgson KO (1983) J Biol Chem 258:12761–12764
21. Groves JT, McMurry TJ (1985) Rev Port Quim 27:102–103
22. Balch AL, Latos-Grazynski L, Renner MW (1985) J Am Chem Soc 107:2983–2985
23. Gross Z, Nimri S (1994) Inorg Chem 33:1731–1732
24. Poulos TL (1996) JBIC 1:356–359
25. Fulop V, Phizackerley RP, Soltis SM, Clifton IJ, Wakatsuki S, Erman J, Hajdu J, Edwards SL (1994) Structure 2:201–208
26. Penner-Hahn JE, Hodgson KO (1989) In: Lever ABP, Gray HB (eds) Physical bioinorganic chemistry, Series 4, Part III, Iron porphyrins. VCH, Weinheim, pp 235–304
27. Paeng KJ, Kincaid JR (1988) J Am Chem Soc 110:7913–7915

28. Oertling WA, Babcock GT (1988) Biochemistry 27:3331–3338
29. Hashimoto S, Teraoka J, Inubishi T, Yonetani T, Kitagawa T (1986) J Biol Chem 261:11110–11118
30. Reczek CM, Sitter AJ, Terner J (1989) J Mol Struct 214:27–41
31. Sitter AJ, Reczek CM, Terner J (1985) J Biol Chem 260:7515–7522
32. Hashimoto S, Mizutani Y, Tatsuno Y, Kitagawa T (1991) J Am Chem Soc 113:6542–6549
33. Groves JT, McClusky GA (1976) J Am Chem Soc 98:859–861
34. Groves JT, Gross Z (1995) In: Kessissoglou DP (ed) Bioinorganic chemistry: an inorganic perspective of life (NATO ASI Series, vol 459). Kluwer, Dordrecht, pp 39–47
35. Groves JT, Avaria-Neisser GE, Fish KM, Imachi M, Kuczkowski RL (1986) J Am Chem Soc 108:3837–3838
36. Collman JP, Brauman JI, Hampton PD, Tanaka H, Bohle DS, Hembre RT (1990) J Am Chem Soc 112:7980
37. Arasasingham RD, He GX, Bruice TC (1993) J Am Chem Soc 115:7985–7991
38. Traylor TG (1991) Pure Appl Chem 63:265–274
39. Rietjens IMCM, Osman AM, Veeger C, Zakharieva O, Antony J, Grodzicki M, Trautwein AX (1996) JBIC 1:372–376
40. Khenkin AM, Hill CL (1993) J Am Chem Soc 115:8178–8186
41. Groves JT, Watanabe Y (1986) J Am Chem Soc 108:507–508
42. Gross Z, Nimri S (1995) J Am Chem Soc 117:8021–8022
43. Czarnecki K, Nimri S, Gross Z, Proniewicz LM, Kincaid JR (1996) J Am Chem Soc 118:2929–2935
44. Gross Z, Nimri S, Simkhovich L (1996) J Mol Cat A: Chem 113:231–238
45. Groves JT, Gross Z, Stern MK (1994) Inorg Chem 33:5065–5072
46. Gans P, Buisson G, Duee E, Marchon J-C, Erler BS, Scholz WF, Reed CA (1986) J Am Chem Soc 108:1223–1234
47. Kaustov L, Tal ME, Shames AI, Gross Z (1997) Inorg Chem 36:in press
48. Sisemore MF, Burstyn JN, Valentine JS (1996) Angew Chem Int Ed Eng 35:206–208, Angew Chem 108:195–196
49. Machii K, Watanabe Y, Morishima I (1995) J Am Chem Soc 117:6691–6697
50. Groves JT, Quinn R, McMurry TJ, Nakamura M, Lang G, Boso B (1985) J Am Chem Soc 107:354–360
51. Sugitomo H, Tung H, Sawyer DT (1988) J Am Chem Soc 110:2465–2470
52. Barzilay CM, Sibilia SA, Spiro TG, Gross Z (1995) Chem Eur J 1:222–231
53. Groves JT, Watanabe Y (1986) J Am Chem Soc 108:7836–7837
54. La Mar GN, Walker FA (1979) In: Dolphin D (ed) The porphyrins, vol 4. Academic, New York, pp 61–157
55. Toney GE, terHaar LW, Savrin JE, Gold A, Hatfield WE, Sangaiah R (1984) Inorg Chem 23:2561–2563
56. Reed CA, Guiset F (1996) J Am Chem Soc 118:3281–3282
57. Turner P, Gunter MJ (1994) Inorg Chem 33:1406–15
58. Basolo F, Pearson RG (1962) Prog Inorg Chem 4:381–453
59. Chapman NB, Shorter J (1972) Advances in linear free energy relationships. Plenum, New York
60. Gross Z, Kaustov L (1995) Tetrahedron Lett 36:3735–3736
61. Swistak C, Mu XH, Kadish KM (1987) Inorg Chem 26:4360–4366
62. Ostovic D, Bruice TC (1989) J Am Chem Soc 111:6511–6517
63. Spreer LO, Maliyackel AC, Otros JW, Melvin C (1987) Inorg Chem 26:4133–5
64. Camenzind MJ, Hollander FJ, Hill CL (1982) Inorg Chem 21:4301–4308
65. Hickman DL, Nanthakumar A, Goff HM (1988) J Am Chem Soc 110:6384–6390
66. Watabe T, Akamatsu K (1974) Biochem Pharmacol 23:1079–1085
67. Groves JT, Nemo TE, Myers RS (1979) J Am Chem Soc 101:1032–1033
68. Collman JP, Kodadek T, Raybuck SA, Brauman JI, Papazian LM (1985) J Am Chem Soc 107:4343–4345
69. Gross Z, Ini S (1997) J Org Chem 62 (in press)
70. Palucki M, Pospisil PJ, Zhang W, Jacobsen EN (1994) J Am Chem Soc 116:9333–9334
71. Higuchi T, Hirobe M (1996) J Mol Cat A: Chem 113:403–422
72. Gross Z (1996) JBIC 1:372–376
73. Bernardou J, Fabiano A-S, Robert A, Meunier B (1994) J Am Chem Soc 116:9375–9376